ORIGINAL ARTICLE

# Development of a bacteria-nanosapper for the active delivery of ZIF-8 particles containing therapeutic genes for cancer immune therapy

**Yiting Qiao[a,b,c,d,e,†,*], Miao Luo[b,f,†], Yufei Wang[b], Haoxiang Qi[b], Menglan Wang[b], Yunxin Pei[b], Mengqing Sun[b], Zhengguo Zhang[b], Jiacheng Huang[a], Pengyu Gong[b], Shusen Zheng[a,d,e], Jianxiang Chen[b,*]**

[a]*Division of Hepatobiliary and Pancreatic Surgery, Department of Surgery, The First Affiliated Hospital, Zhejiang University School of Medicine, Hangzhou 310003, China*

[b]*School of Pharmacy, Institute of Hepatology and Metabolic Diseases, Department of Hepatology, the Affiliated Hospital of Hangzhou Normal University, Hangzhou Normal University, Hangzhou 311121, China*

[c]*Jinan Microecological Biomedicine Shandong Laboratory, Jinan 250000, China*

[d]*NHC Key Laboratory of Combined Multi-organ Transplantation, Key Laboratory of Organ Transplantation, Hangzhou 310003, China*

[e]*Key Laboratory of the Diagnosis and Treatment of Organ Transplantation, Research Unit of Collaborative Diagnosis and Treatment For Hepatobiliary and Pancreatic Cancer, Chinese Academy of Medical Science (2019RU019), Hangzhou 310003, China*

[f]*Key Laboratory of Digital Technology in Medical Diagnostics of Zhejiang Province, Dian Diagnostics Group Co., Ltd., Hangzhou 310000, China*

Received 17 May 2024; received in revised form15 July 2024; accepted 18 July 2024

*Corresponding authors.

E-mail addresses: chenjx@hznu.edu.cn (Jianxiang Chen), yitingqiao@zju.edu.cn (Yiting Qiao).

[†]These authors made equal contributions to this work.

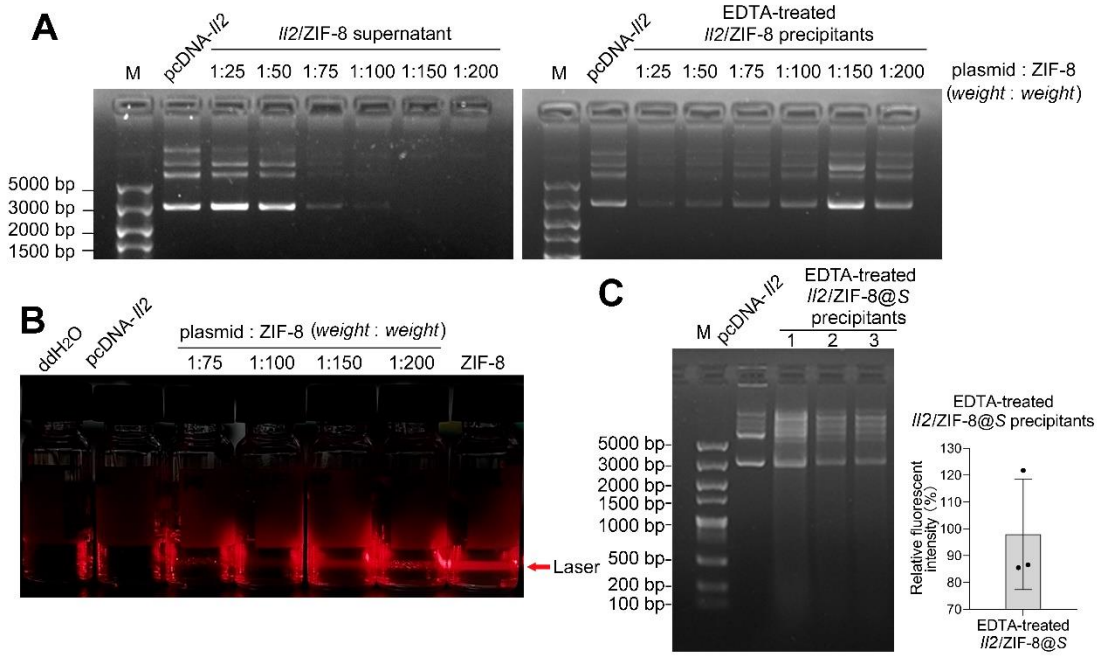


**Figure S1** The design, preparation, characterization and *in vivo* distribution of *Il2*/ZIF-8@*Salmonella* (Related to Fig. 1). (A) Gel electrophoresis images for the supernatants (left) and EDTA-treated precipitants (right) of *Il2*/ZIF-8 particles composed of various ratio of plasmid and ZIF-8 after centrifugal separation. (B) Light scattering phenomenon of aqueous solutions containing various combinations of plasmid and ZIF-8. (C) Gel electrophoresis image for input pcDNA-*Il2* plasmid and EDTA-treated *Il2*/ZIF-8@*Salmonella* precipitants. The gray scale of nucleic acid bands was quantified and shown as histogram.

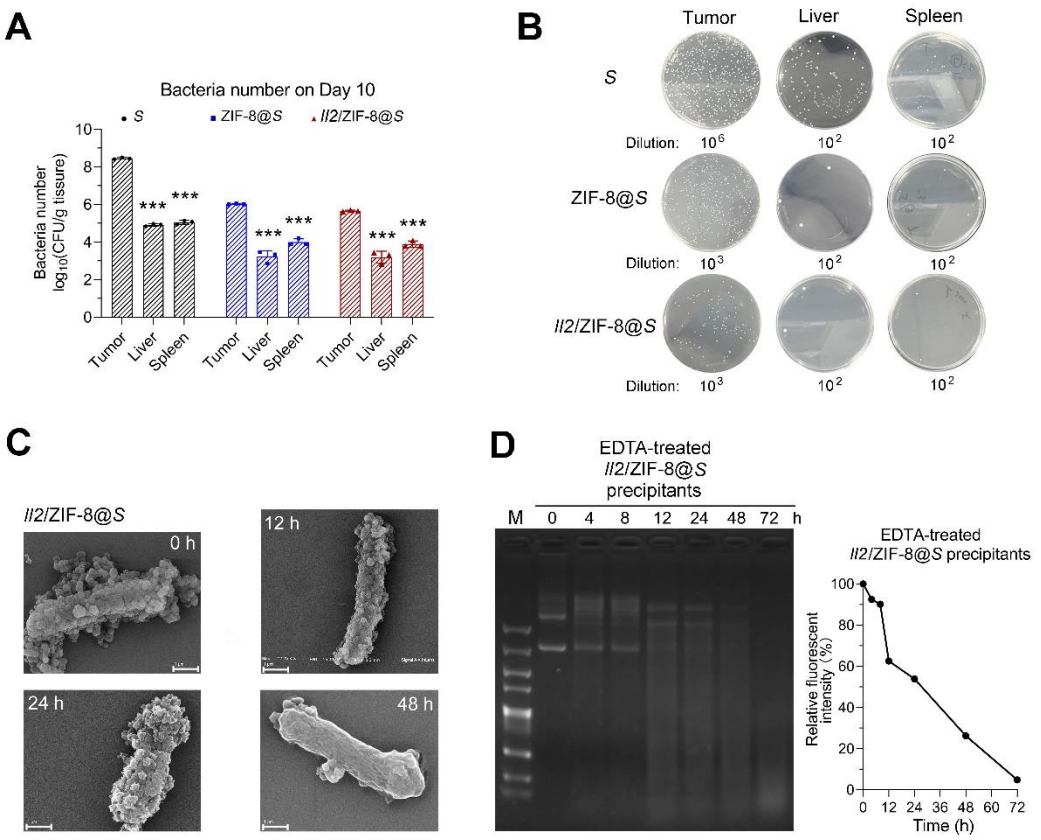


**Figure S2** *In vivo* bacteria distribution assay on Day 10 post-treatment (Related to Fig. 1). (A) Live bacteria titers in the melanoma tumor tissues, livers and spleens on Day 10 after the intravenous injection of *Salmonella*, ZIF-8@*Salmonella,* and *Il2*/ZIF-8@*Salmonella* at the dosage of $10^7$ CFU/mouse. $n = 3$. Data were expressed as mean ± SD. Student' *t* test was carried out using intratumoral titer as control for each treatment regime. ***$P < 0.001$; *ns*, not significant. (B) Representative images of bacterial colonies produced by homogenized melanoma tumor tissues, livers and spleens on Day 10 after the intravenous injection *Salmonella*, ZIF-8@*Salmonella*, and *Il2*/ZIF-8@*Salmonella* at the dosage of $10^7$ CFU/mouse. (C) Representative TEM images of *Il2*/ZIF-8@*Salmonella* kept in PBS at 37 ℃ for indicated durations. Scale bar = 1 μm. (D) Gel electrophoresis image for EDTA-treated *Il2*/ZIF-8@*Salmonella* precipitants kept in PBS at 37 ℃ for indicated durations. The gray scale of nucleic acid bands was quantified and shown as line chart.

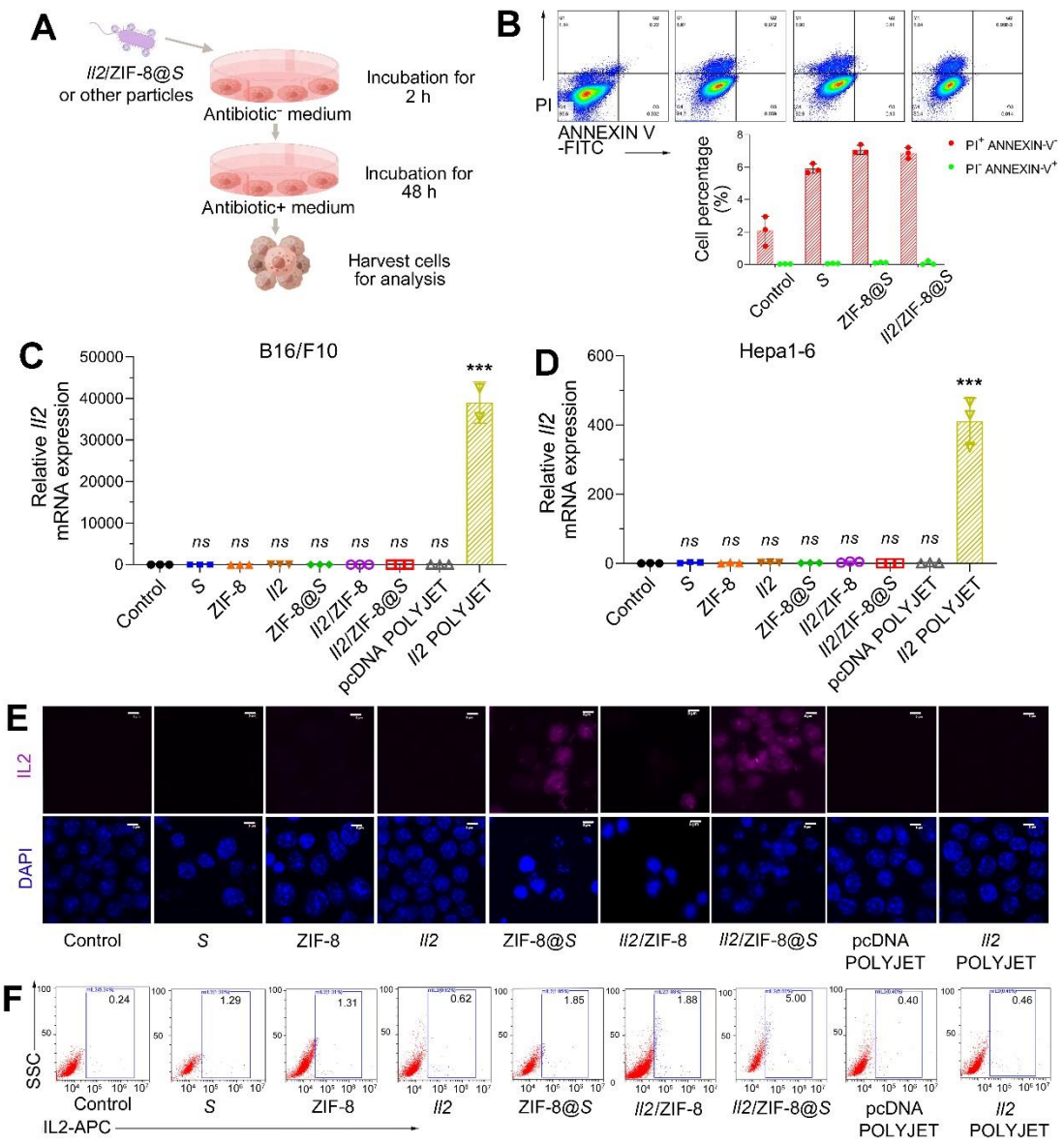


**Figure S3** *In vitro* analysis of gene delivery efficiency of *Il2*/ZIF-8@*Salmonella* in macrophages and tumor cells (Related to Fig. 3). (A) The schematic illustration for the experimental procedures for gene delivery efficiency assay. (B) Apoptosis assay of RAW264.7 cell after 2-h treatment of various regimes followed by 48-h incubation with fresh medium with antibiotics. (C–D) qPCR analysis of B16/F10 (C) and Hepa1-6 (D) cells incubated with indicated particle compositions. $n = 3$. Data were expressed as mean ± SD. Student' $t$ test was carried out using PBS-treated cells as control for each treatment regime. ***$P < 0.001$; *ns*, not significant. (E) Fluorescent images of separated acquisition channels showing IL2 expression in RAW264.7 cells incubated with

indicated particle compositions. Pink represented the signals of APC-labeled anti-mouse IL2 antibody. Blue represented DAPI signals. Scale bars = 5 μm. (**F**) Representative images for the flow cytometry analysis of IL2 expression in BMDM cells incubated with indicated particle compositions.

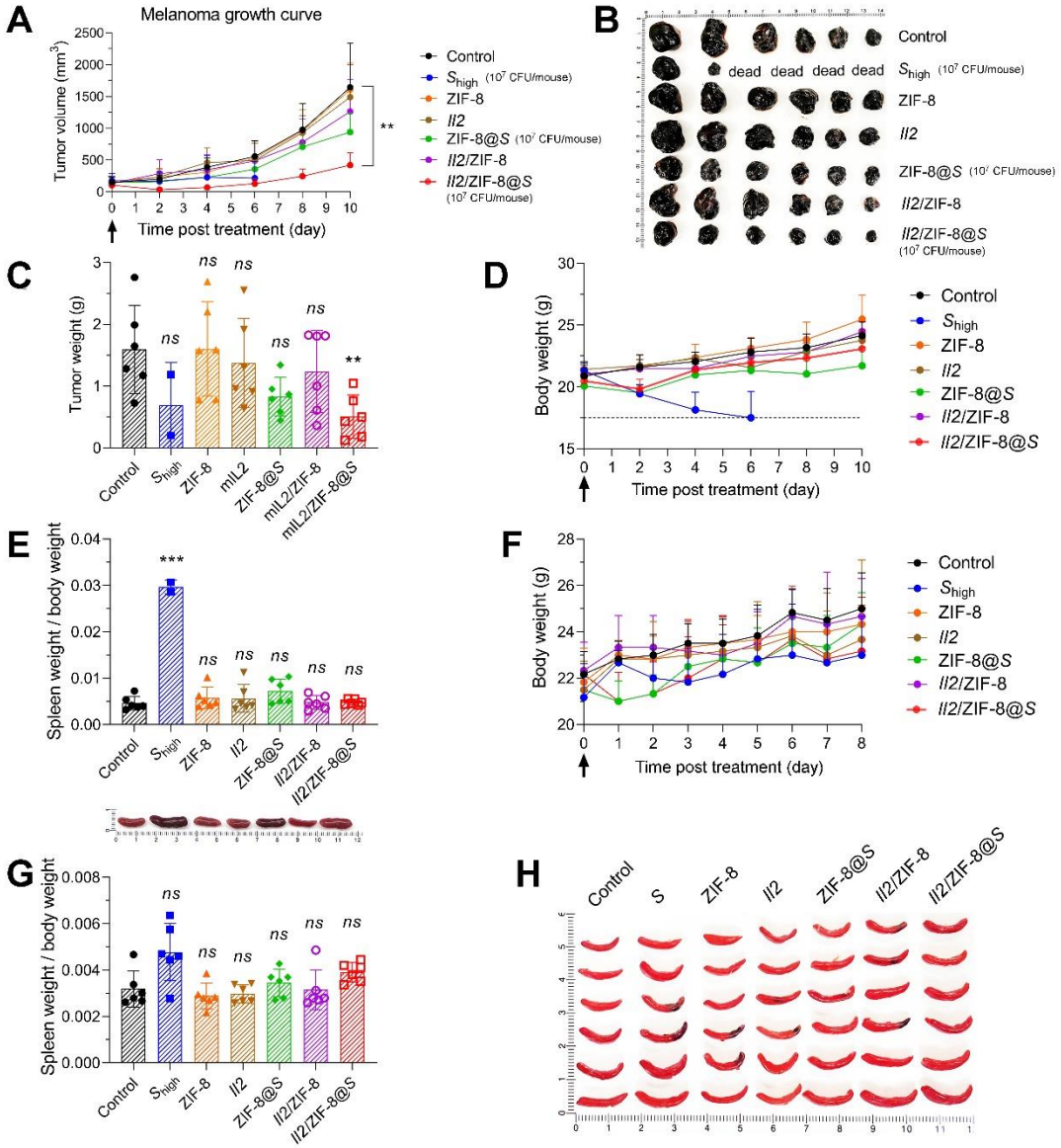


**Figure S4** *In vivo* analysis of therapeutic efficacy of *Il2*/ZIF-8@*Salmonella* in murine melanoma model (Related to Fig. 4). (A) The tumor growth curves for mice treated with one dose of various regimes. $S_{high}$ indicated $10^7$ CFU *Salmonella*/mouse in this figure and successive figures. $n = 6$. Data were expressed as mean ± SD. Student' *t* test was carried out using PBS-treated group as control for each treatment regime. $^{**}P < 0.01$. (B) The image of resected melanomas. (C) The histogram showing tumor weights for groups treated with indicated regimes. $n = 6$. Data were expressed as mean ± SD. Student' *t* test was carried out using PBS-treated group as control for each treatment regime. $^{**}P < 0.01$; *ns*, not significant. (D) The curves of body weights for mice treated with one dose of various regimes. $n = 6$. Data were expressed as mean ± SD. The dotted

line indicated 15% reduction. (E) The histogram showing the ratio of spleen weight and body weight for mice treated with one dose of various regimes. $n$ = 6. Data were expressed as mean ± SD. Student' $t$ test was carried out using PBS-treated cells as control for each treatment regime. ***$P < 0.001$; *ns*, not significant. (F) The curves of body weight for mice treated with one dose of various regimes. $n$ = 6. Data were expressed as mean ± SD. (G) The histogram showing the ratio of spleen weight and body weight for mice treated with one dose of various regimes. $n$ = 6. Data were expressed as mean ± SD. Student' $t$ test was carried out using PBS-treated cells as control for each treatment regime. *ns*, not significant. (H) The image of spleens of mice treated with one dose of various regimes.

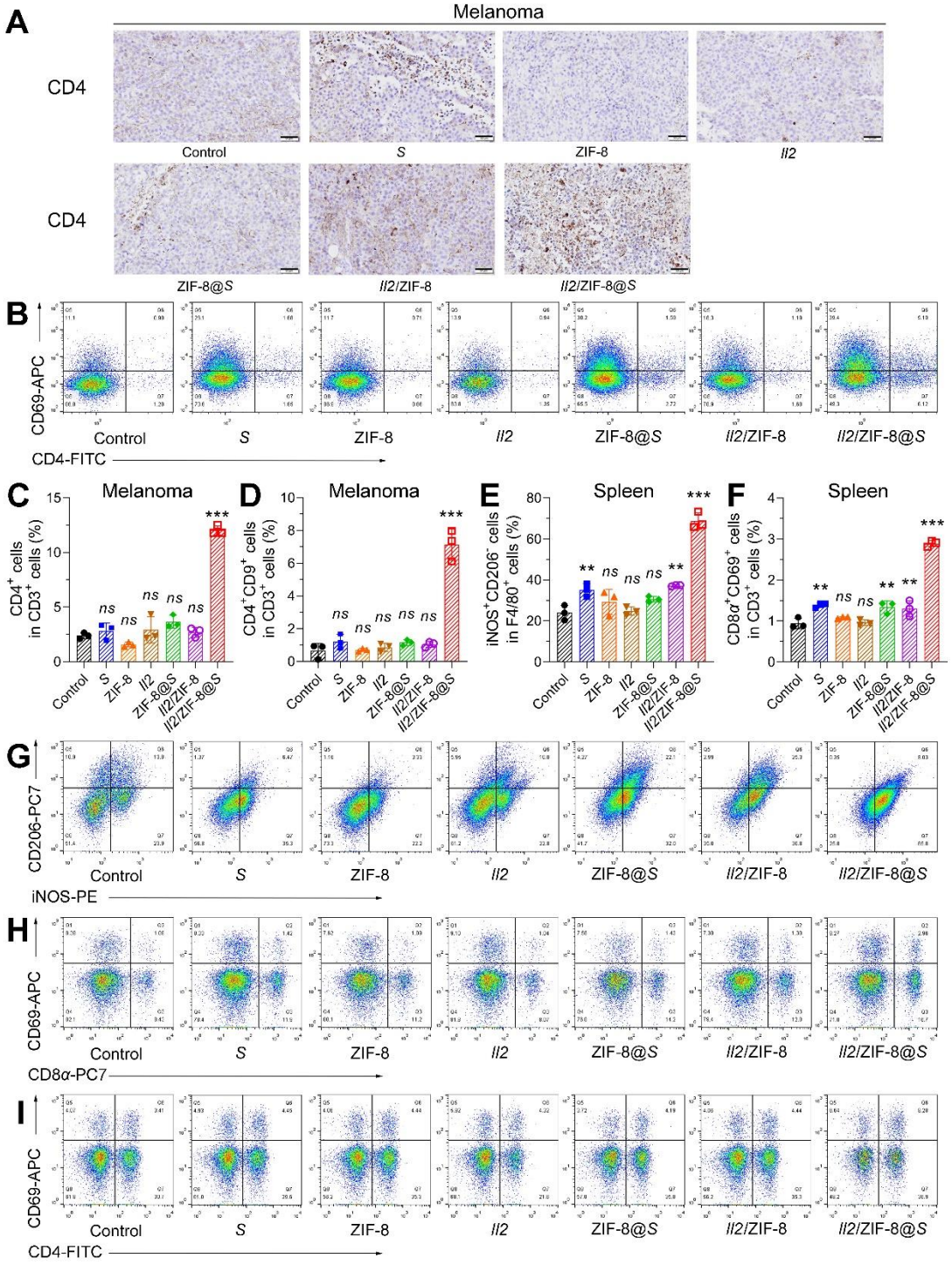


**Figure S5** The analysis of anti-tumor immune responses induced by *Il2*/ZIF-8@*Salmonella* in murine melanoma model (Related to Fig. 5). (A) The representative IHC results showing the CD4 in melanomas treated with indicated regimes. Scale bars = 50 μm. (B) Representative images for the flow cytometry analysis of CD4 and CD69 expression in $CD45^+CD3^+$ intratumoral lymphocytes. (C–D) The histograms showing the percentage of $CD4^+$ cells in $CD3^+$ lymphocytes (C) and $CD4^+CD69^+$ cells in $CD3^+$

lymphocytes (D) in melanomas treated with indicated regimes. $n$ = 3. Data were expressed as mean ± SD. Student' $t$ test was carried out using PBS-treated group as control for each treatment regime. ***$P$ < 0.001; *ns*, not significant. (E–F) The histograms showing the percentage of $iNOS^{+}CD206^{-}$ cells in $F4/80^{+}$ cells (E) and $CD8\alpha^{+}CD69^{+}$ cells in $CD3^{+}$ lymphocytes (F) in spleens treated with indicated regimes. $n$ = 3. Data were expressed as mean ± SD. Student' $t$ test was carried out using PBS-treated group as control for each treatment regime. **$P$ < 0.01; ***$P$ < 0.001; *ns*, not significant. (G–I) Representative images for the flow cytometry analysis of CD206 and iNOS expression in $CD45^{+}F4/80^{+}$ cells (G), CD8$\alpha$ and CD69 expression in $CD45^{+}CD3^{+}$ lymphocytes (H), and CD4 and CD69 expression in $CD45^{+}CD3^{+}$ lymphocytes (I) in spleens for mice treated with indicated regimes.

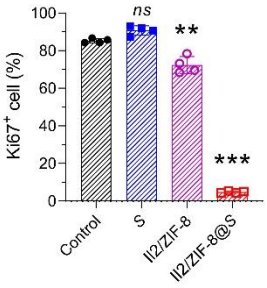


**Figure S6** The percentage of Ki67$^{+}$ cells for orthotopic HCC tissues (Related to Fig. 6)**.** $n$ = 4. Data were expressed as mean ± SD. Student' $t$ test was carried out using PBS-treated group as control for each treatment regime. **$P$ < 0.01; ***$P$ < 0.001; *ns*, not significant.

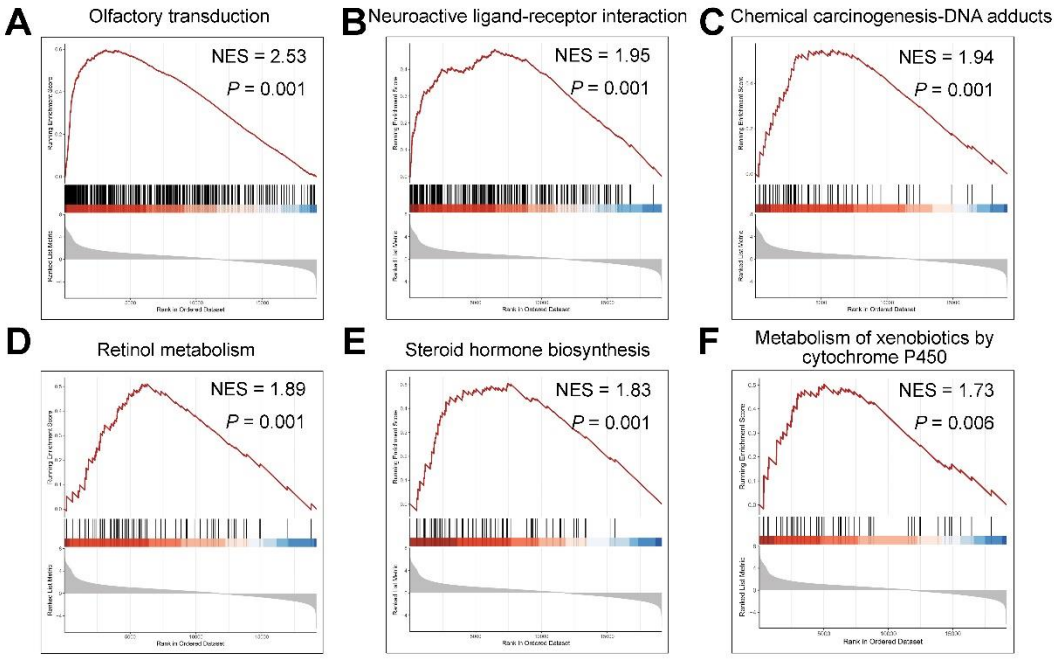


**Figure S7** Single-cell RNA sequencing analysis of cryopreserved HCC tissues after the treatment of *Il2*/ZIF-8@*Salmonella* (Related to Fig. 7). (A-F) GSEA plot of "Olfactory transduction" (A), "Neuroactive ligand-receptor interaction" (B), "Chemical carcinogenesis-DNA adducts" (C), "Retinol metabolism" (D), "Steroid hormone biosynthesis" (E), "Metabolism of xenobiotics by cytochrome P450" (F) gene clusters by comparing the gene expression patterns between Kupffer cells in HCC tissues treated with *Il2*/ZIF-8@*Salmonella* and *Salmonella*.

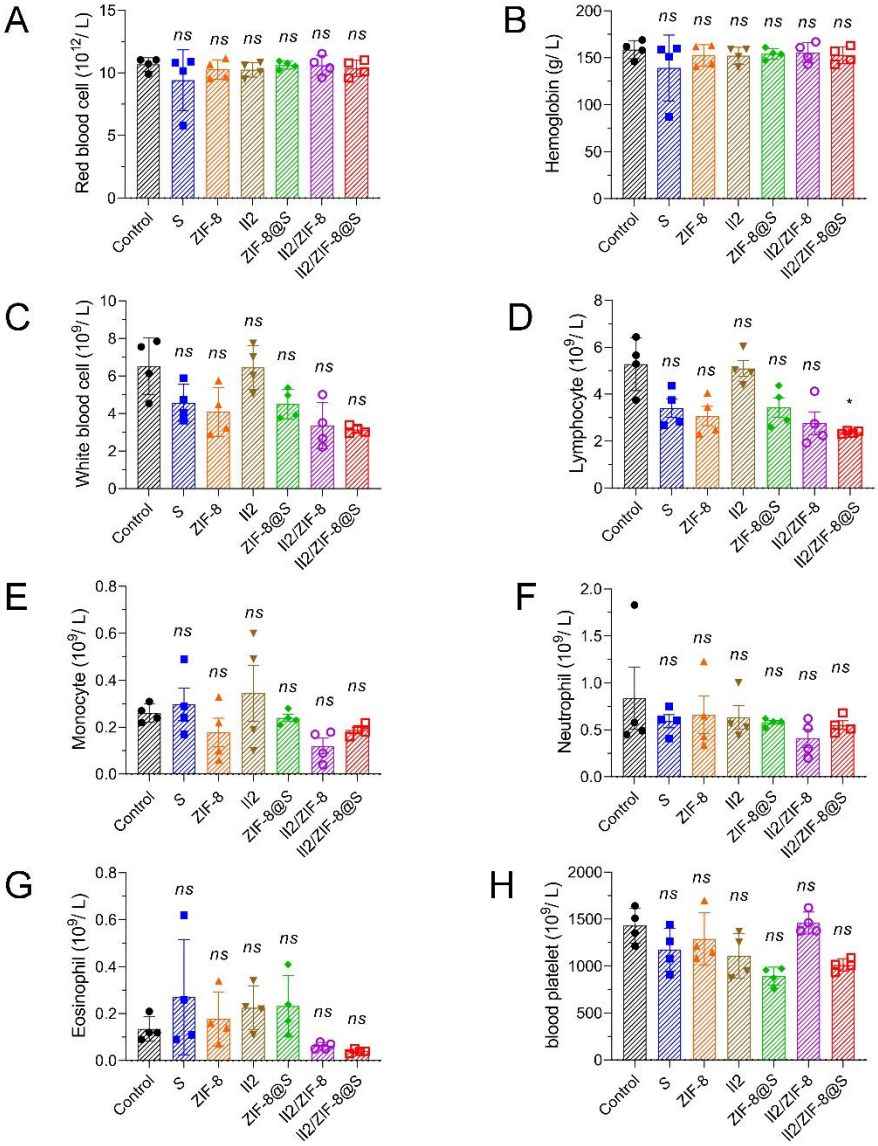


**Figure S8** The analysis for the toxicity of *Il2*/ZIF-8@*Salmonella* to hematopoietic system on Day 8 after treatment (Related to Fig. 8). (A–H) Peripheral blood cell indexes for red blood cells (A), hemoglobin (B), white blood cells (C), lymphocytes (D), monocytes (E), neutrophil (F), eosinophil (G), and blood platelet (H) for mice treated with indicated regimes. $n = 4$. Data were expressed as mean ± SD. Student' *t* test was carried out using PBS-treated group as control for each treatment regime. $^*P < 0.05$; *ns*, not significant.